Hydraulics of Dams and River Structures – Yazdandoost & Attari (eds)
© 2004 Taylor & Francis Group, London, ISBN 90 5809 632 7

Air–water flows in water engineering and hydraulic structures. Basic processes and metrology

H. Chanson
Dept. of Civil Eng., The University of Queensland, Brisbane, Australia

ABSTRACT: Hydraulic researchers had been leading air–water flow studies until the mid-1950s. Since progresses have been dominated by multiphase flow experts despite the relevance of "white water" phenomena to hydraulic engineering. In this lecture the writer reviews the basic mechanisms of air entrainment: singular aeration and interfacial entrainment. The relevant instrumentation and data processing technique are detailed. Later recent progresses in unsteady flow measurements and in seawater are discussed.

1 INTRODUCTION

In Nature, air–water flows are commonly encountered at waterfalls, in mountain torrents and at wave breaking. "White waters" are also observed in aesthetical fountains and in hydraulic structures (e.g. PLUMPTRE 1993, CHANSON 1997) (Fig. 1). One of the first scientific accounts was made by LEONARDO DA VINCI (AD 1452–1519). He described numerous flow situations and he commented the entrainment of air at waterfalls, plunging jet flows, drop structures, running waters, breaking waves, calling the air–water mixture foam (*schiuma*) and white waters (*bianchezza*). He was intrigued by air entrainment when waters plunge into a receiving pool of water: "Where the water issues forth from the said pool (…) falling or descending through the air, this water acquires weight and impetus; and then piercing the water where it strikes, it tears it apart and dives down

Figure 1. Air entrainment at Chinchilla weir (Australia) – Note self-aeration down chute and in hydraulic jump (foreground) – The beige colour of water is caused by three-phase mixing (air, water & sediment).

in fury (…) accompanied by the air which has been submerged with it"; "If (…) air is submerged with impetus it comes back out of the water"; "Air can never of itself remain beneath the water but always wishes to be above" (McCURDY 1956, Vol. 2). LEONARDO DA VINCI recognised with discernment that air entrainment at plunging jet is related to the momentum ("impetus") of impinging flow. Recent studies highlighted indeed that the impact velocity of the plunging jet is a dominant parameter (WOOD 1991, CHANSON 1997).

Air–water flows have been studied recently compared to classical fluid mechanics. Although some researchers observed free-surface aeration and discussed possible effects (e.g. STEWART 1913), the first successful experimental investigations were conducted during the mid-20th century (CHANSON 1997, HAGER and KRAMER 2003). That is, EHRENBERGER (1926) in Austria, and STRAUB and ANDERSON (1958) in North-America. The latter data set is still widely used by engineers and researchers: e.g., it was cited 24 times between 1985 and June 2001 in Science Citation Index Expanded™. Another important work was the series of experiments performed on the Aviemore dam spillway in New Zealand (KELLER 1972, CAIN 1978) under the supervision of I.R. WOOD. Laboratory and prototype experimental investigations showed the complexity of the free-surface aeration process. Ian R. WOOD further developed the basic principles of modern self-aerated flow calculations. In particular, the uniform equilibrium air–water flow properties (WOOD 1983), the air content and mean velocity distributions (CAIN and WOOD 1981, WOOD 1984) and the gradually-varied air–water flow properties (WOOD 1985).

These significant findings are not complete and the contribution of hydraulic engineers to gas–liquid flow research has been relatively modest for the last 40 years. Fundamental research has been dominated by chemical, mechanical and nuclear engineers. For example, the intrusive phase-detection needle probe design was developed by Professor S.G. BANKOFF (NEAL and BANKOFF 1963); phase detection optical fibre probes were developed in the late 1960s (JONES and DELHAYE 1976) despite dubious claims! For the period 1985–2003, hydraulic and civil engineering researchers contributed less than 3% of all publications in International Journal of Multiphase Flow. In 2004, hydraulic professionals and researchers lack advanced multiphase flow expertise. In the following paragraphs, the basic mechanisms of air entrainment are discussed and new advances in air–water flows are presented.

2 FREE-SURFACE AERATION IN TURBULENT FLOWS: BASIC MECHANISMS

2.1 *Basic definitions*

Air entrainment, or free-surface aeration, is defined as the entrainment/entrapment of undissolved air bubbles and air pockets that are carried away within the flowing fluid. The resulting *air–water mixture* consists of both air packets within water and water droplets surrounded by air. It includes also spray, foam and complex air–water structures. In *turbulent flows*, there are two basic types of air entrainment process. The entrainment of air packets can be localised or continuous along the air–water interface (Fig. 2). Examples of *local aeration* include air entrainment by plunging jet and at hydraulic jump (Fig. 1). Air bubbles are entrained locally at the intersection of the impinging jet with the surrounding waters (Fig. 2 Top). The intersecting perimeter is a singularity in terms of both air entrainment and momentum exchange, and air is entrapped at the discontinuity between the high-velocity jet flow and the receiving pool of water. *Interfacial aeration* (or continuous aeration) is defined as the air entrainment process along an air–water interface, usually parallel to the flow direction: e.g., in chute flows (Fig. 1 Left, Fig. 2 Middle). An *intermediate case* is a high-velocity water jets discharging into air. The nozzle is a singularity, characterised by a high rate of aeration, followed by some interfacial aeration downstream at the jet free-surfaces (Fig. 2 Bottom).

2.2 *Local (singular) aeration mechanism: air entrapment at plunging jets*

With local (singular) aeration, air entrainment results from some discontinuity at the impingement perimeter: e.g., plunging water jets, hydraulic jump flows. One basic example is the vertical plunging jet (Fig. 2 Top). At plunge point, air may be entrapped when the impacting flow conditions exceeding a critical threshold (McKEOGH 1978, ERVINE et al. 1980, CUMMINGS and CHANSON 1999). McKEOGH (1978) showed first that the flow conditions at *inception of air entrainment* are functions of the jet turbulence level. For a given plunging jet configuration, the

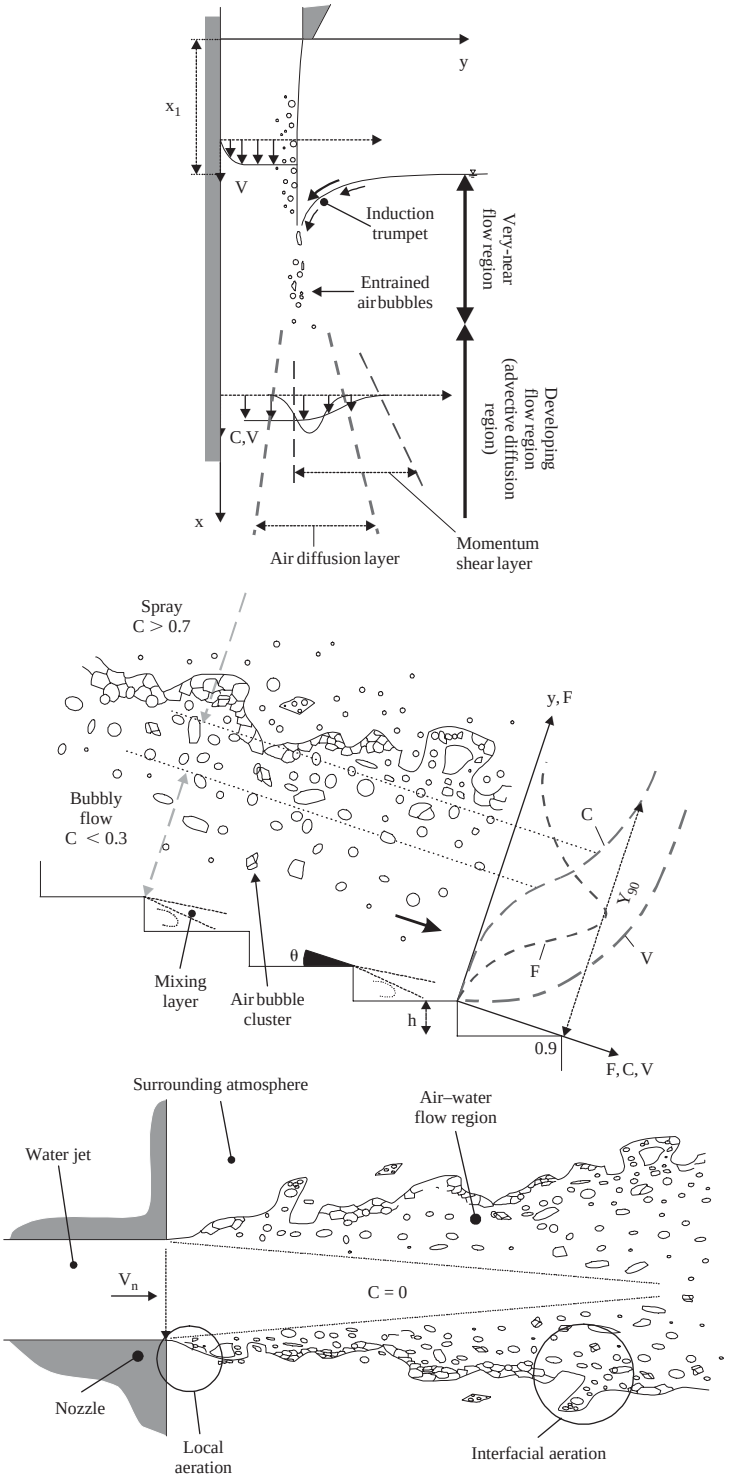

Figure 2. Sketch of basic free-surface aeration processes.

onset velocity increases with decreasing jet turbulence. For vertical water jets, the dimensionless onset velocity may be correlated by:

$$\frac{V_e * \mu_w}{\sigma} = 0.0109 * (1 + 3.375 * \exp(-80 * Tu)) \quad (1)$$

where V_e is the onset velocity, μ_w is the liquid dynamic viscosity, σ is the surface tension and Tu is the ratio of the standard deviation of the jet velocity fluctuations about the mean to the jet impact velocity (CUMMINGS and CHANSON 1999).

For jet impact velocities slightly larger than the onset velocity, air is entrained in the form of *individual bubbles and packets*. The entrained air may have the form of "kidney-shaped" bubbles which may break up into two "daughter" bubbles, "S-shape" packets, or elongated "finger" that may break-up to form several small bubbles by a tip-streaming mechanism, depending upon the initial size of the entrained air packet. The air entrainment rate is very small, hardly measurable with phase detection intrusive probes. At higher impact velocities, the amount of entrained air becomes significant and the air diffusion layer is clearly marked by the *white plume* generated by the entrained bubbles. Air entrainment is an unsteady, rapidly-varied process. An *air cavity is set into motion* between the impinging jet and the surrounding fluid and it is stretched by turbulent shear (Fig. 3). The air cavity behaves as a ventilated air sheet and air pockets are entrained by discontinuous gusts at the lower tip of the elongated air cavity. Initial aeration of the impinging jet free-surface may further enhance the process (VAN DE SANDE and SMITH 1973, BRATTBERG and CHANSON 1998).

In the very-near flow field (i.e. $(x - x_1)/d_1 < 5$), the flow is dominated by air entrapment and the interactions between gas and liquid entrainment (Fig. 3). Dominant flow features include an *induction trumpet* generated by the liquid entrainment and the *elongated air cavity* at jet impingement (thickness δ_{al}). Experimental observations showed that the air entrapment/entrainment process is very dynamic and it interacts substantially with the transfer of momentum across the mixing layer. There is a distinct discontinuity between the impinging jet flow and the induction trumpet as sketched in Figure 3 which shows an instantaneous "snapshot" of the entrapment region. Experimental data indicated a velocity discontinuity across the elongated air cavity: $V_i \propto (V_1 - V_e)^{0.15}$, where V_1 is the jet impact velocity and V_i is the liquid entrainment velocity in the induction trumpet (CHANSON 2002). It is believed that air entrainment takes place predominantly in the elongated cavity by a Couette flow motion (Fig. 3 Right). For two-dimensional plunging jets, the air entrainment rate q_{air} may be estimated as:

$$q_{air} = \int_{d_1}^{d_1+\delta_{al}} V_{air} * \, dy \approx \frac{V_1 + V_i}{2} * \delta_{al} \quad (2)$$

Downstream of the entrapment region (i.e. $(x - x_1)/d_1 > 5$), the distributions of void fractions exhibit smooth, derivative profiles which follow closely simple analytical solutions of the advective

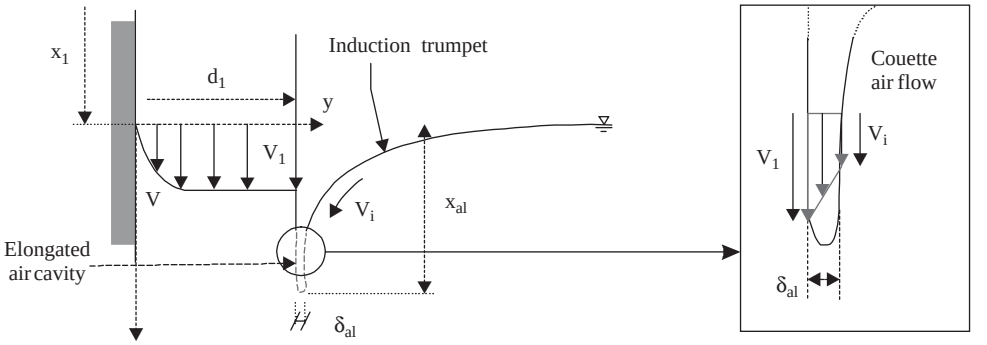

Figure 3. Detail of the air entrapment region and the very-near flow field.

diffusion equation for air bubbles (CHANSON 1997). For two-dimensional vertical jets, it yields:

$$C = \frac{\frac{Q_{air}}{Q_w}}{\sqrt{4 * \pi * D^{\#} * \frac{x - x_1}{Y_{C_{max}}}}} * \left(\exp\left(-\frac{\left(\frac{y}{Y_{C_{max}}} - 1\right)^2}{4 * D^{\#} * \frac{x - x_1}{Y_{C_{max}}}} \right) + \exp\left(-\frac{\left(\frac{y}{Y_{C_{max}}} + 1\right)^2}{4 * D^{\#} * \frac{x - x_1}{Y_{C_{max}}}} \right) \right) \quad (3)$$

where $D^{\#}$ is a dimensionless air bubble diffusivity and $Y_{C_{max}} = y(C = C_{max})$. CUMMINGS and CHANSON (1997) and BRATTBERG and CHANSON (1998) presented successful comparisons between Equation (3) and experimental data. With circular plunging jets, the analytical solution of the diffusion equation becomes:

$$C = \frac{Q_{air}}{Q_w} * \frac{1}{4 * D^{\#} * \frac{x - x_1}{Y_{C_{max}}}} * \exp\left(-\frac{1}{4 * D^{\#}} * \frac{\left(\frac{r}{Y_{C_{max}}}\right)^2 + 1}{\frac{x - x_1}{Y_{C_{max}}}} \right) * I_0 \left(\frac{1}{2 * D^{\#}} * \frac{\frac{r}{Y_{C_{max}}}}{\frac{x - x_1}{Y_{C_{max}}}} \right) \quad (4)$$

where I_0 is the modified Bessel function of the first kind of order zero. CHANSON and MANASSEH (2003) and CHANSON et al. (2002) showed successful comparisons between Equation (4) and experimental data.

2.3 *Interfacial aeration process: self-aeration down a steep chute*

Examples of interfacial aeration include spillway flows and "white waters" down a mountain stream (Fig. 1, 2 Middle and 4). On smooth and stepped (skimming flow) chutes, the upstream flow is non-aerated but free-surface instabilities are observed. Such wave instabilities were mentioned by ANWAR (1994), CHANSON (1997) and MATOS et al. (1999) for example. The location of inception of free-surface aeration is clearly defined however (Fig. 4). Downstream the flow becomes rapidly aerated. Self aeration may induce significant flow bulking, air–water mass transfer drag reduction while it may prevent cavitation damage (FALVEY 1980,1990, WOOD 1983, CHANSON 1994).

KEULEGAN and PATTERSON (1940) analysed wave instability and implied that air bubbles may be entrained by a breaking wave mechanism at the free surface. Photographs by CAIN (1978) at Aviemore dam spillway showed that air is entrained by the action of a multitude of irregular vortices

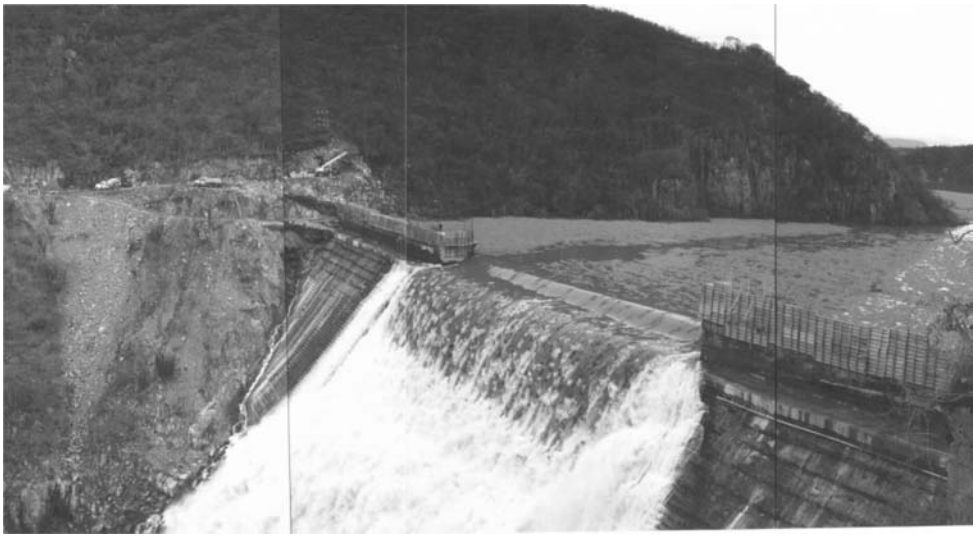

Figure 4. Skimming flow down Trigomil stepped spillway (Mexico): $Q_w = 1,017\,m^3/s$, chute width: 75 m (Courtesy of Drs Sanchez-Bribiesca and Gonzales-Villareal).

acting next to the free-surface. Basically air bubble entrainment is caused by turbulence fluctuations acting next to the air–water free surface. Through the "free-surface", air is continuously trapped and released. Air bubbles may be entrained when the turbulent kinetic energy is large enough to overcome both surface tension and gravity effects. The turbulent velocity be greater than the surface tension pressure and the bubble rise velocity component for the bubbles to be carried away:

$$v' > \text{Maximum}\left(\sqrt{\frac{8 * \sigma}{\rho_w * d_{ab}}}; u_r * \cos\theta\right) \quad (5)$$

where v' is an instantaneous turbulent velocity normal to the flow direction, σ is the surface tension, ρ_w is the water density, d_{ab} is the diameter of the entrained bubble, u_r is the bubble rise velocity and θ is the channel slope (ERVINE and FALVEY 1987, CHANSON 1993). Equation (5) predicts the occurrence of air bubble entrainment for $v' > 0.1$ to 0.3 m/s. The condition is nearly always achieved in prototype chute flows because of the strong turbulence generated by boundary friction. Interfacial aeration involves both the entrainment of air bubbles and the formation of water droplets. The air–water mixture flow consists of water surrounding air bubbles (C < 30%), air surrounding

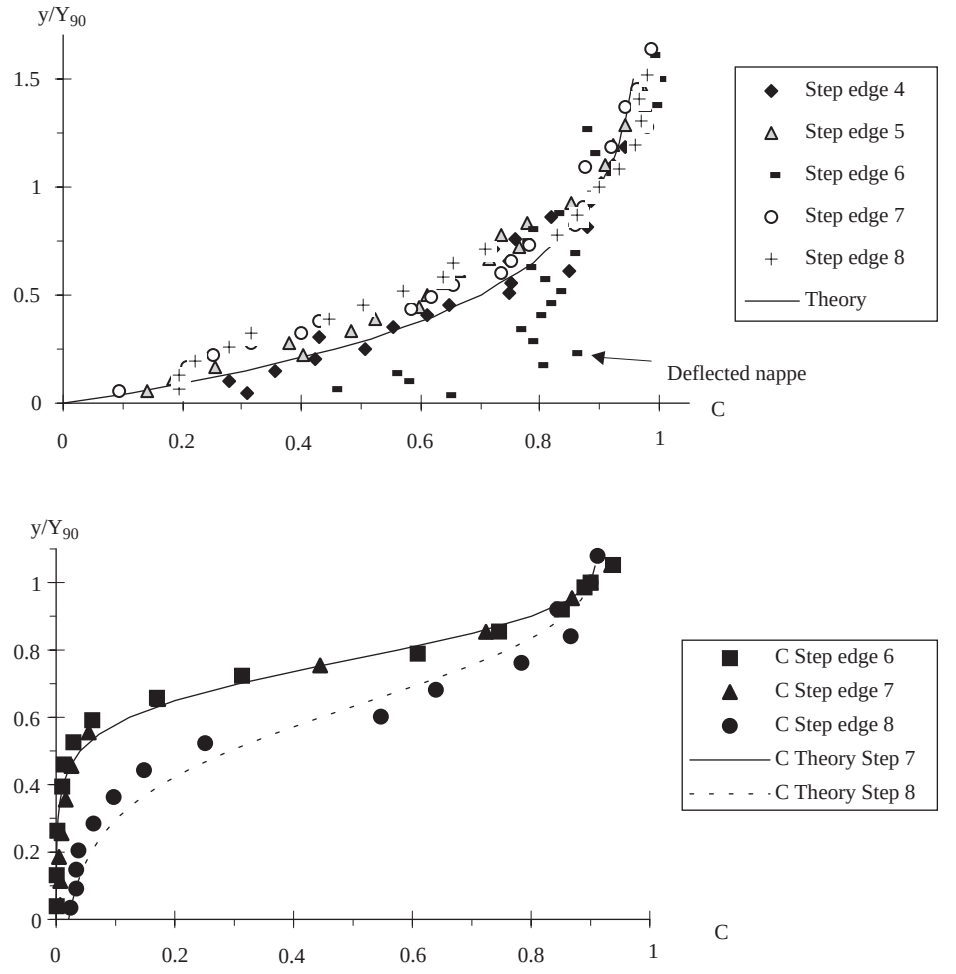

Figure 5. Dimensionless distributions of void fraction in stepped chute flow ($\theta = 21.8°$, step height: 0.1 m, chute width: 1 m). Top: Transition flow, $q = 0.058\ m^2/s$ (data measured at outer step edges) – Comparison with Equation (6). Bottom: Skimming flow: $q = 0.182\ m^2/s$ (data measured at outer step edges) – Comparison with Equation (7).

water droplets (C > 70%) and an intermediate flow structure for 0.3 < C < 0.7 (Fig. 2 Middle). (REIN (1998) and CHANSON (1999) discussed specifically the spray region (i.e. C > 95%).) Note that waves and wavelets propagate downstream along the free-surface. A phase detection probe, fixed in space, will record a fluctuating signal corresponding to both air–water structures and wave passages, adding complexity of the interpretation of the signal (TOOMBES 2002).

Downstream of the inception point of free-surface aeration, air and water are fully mixed, forming a homogeneous two-phase flow (CHANSON 1995, 1997). The advective diffusion of air bubbles may be described by simple analytical models. In transition flows down a stepped chute, the distributions of void fraction follow closely:

$$C = K' * \left(1 - \exp\left(-\lambda * \frac{y}{Y_{90}}\right)\right) \quad \text{Transition flows} \tag{6}$$

where y is distance measured normal to the pseudo-invert, Y_{90} is the characteristic distance where $C = 90\%$, K' and λ are dimensionless function of the mean air content only. Equation (6) compared favourably with experimental data (CHANSON and TOOMBES 2002) (Fig. 5 Top).

In skimming flows and smooth-chute flows, the air concentration profiles have a S-shape that may be modelled by:

$$C = 1 - \tanh^2\left(K' - \frac{\frac{y}{Y_{90}}}{2D_0} + \frac{\left(\frac{y}{Y_{90}} - \frac{1}{3}\right)^3}{3 * D_0}\right) \quad \text{Skimming \& smooth-chute flows} \tag{7}$$

where K' is an integration constant and D_0 is a function of the mean void fraction only. In Figure 5 (Bottom), laboratory data are compared successfully with Equation (7). Although Figure 5 highlights different shapes of void fraction distribution between transition and skimming flows, Equations (6) and (7) derive from the same basic equation assuming different diffusivity profiles (CHANSON and TOOMBES 2002).

3 BASIC METROLOGY IN HYDRAULIC ENGINEERING

In hydraulic engineering, classical measurement devices (e.g. Pitot tube, LDV) are affected by entrained bubbles and might lead to inaccurate readings. When the void fraction C exceeds 5 to 10%, and is less than 90 to 95%, the most robust instrumentation is the intrusive phase detection probes: optical fibre probe and conductivity/resistivity probe (JONES and DELHAYE 1976, BACHALO 1994, CHANSON 1997,2002). The intrusive probe is designed to pierce bubbles and droplets (Fig. 6A). For example, the probe design shown in Figure 6A was designed with a small frontal area of the first tip and with a displaced second tip (offset < $0.2 * \Delta x$) to avoid wake disturbance from the leading tip. Tests showed the absence of wake disturbance during all the experiments (CHANSON 1995). A typical probe signal output is shown in Figure 6B. Although the signal is theoretically rectangular, the probe response is not exactly square because of the finite size of the tip, the wetting/drying time of the interface covering the tip and the response time of the probe and electronics (e.g. CUMMINGS 1996).

3.1 *Data processing*

The basic probe outputs are the void fraction, bubble count rate and bubble chord time distributions with both single-tip and double-tip probe designs. The void fraction C is the proportion of time that the probe tip is in the air. The bubble count rate F is the number of bubbles impacting the probe tip. The bubble chord times provide information on the air–water flow structure. For one-dimensional flows, chord sizes distributions may be derived (e.g. CHANSON et al. 2002).

A dual-tip probe design (Fig. 6A) provides additionally the air–water velocity, specific interface area, chord length size distributions and turbulence level. The velocity measurement is based upon the successive detection of air–water interfaces by two tips. In turbulent air–water flows, the successive detection of all bubbles by each tip is highly improbable and it is common to use a cross-correlation technique (e.g. CROWE et al. 1998). The time-averaged air–water velocity equals:

$$V = \frac{\Delta x}{T} \tag{8}$$

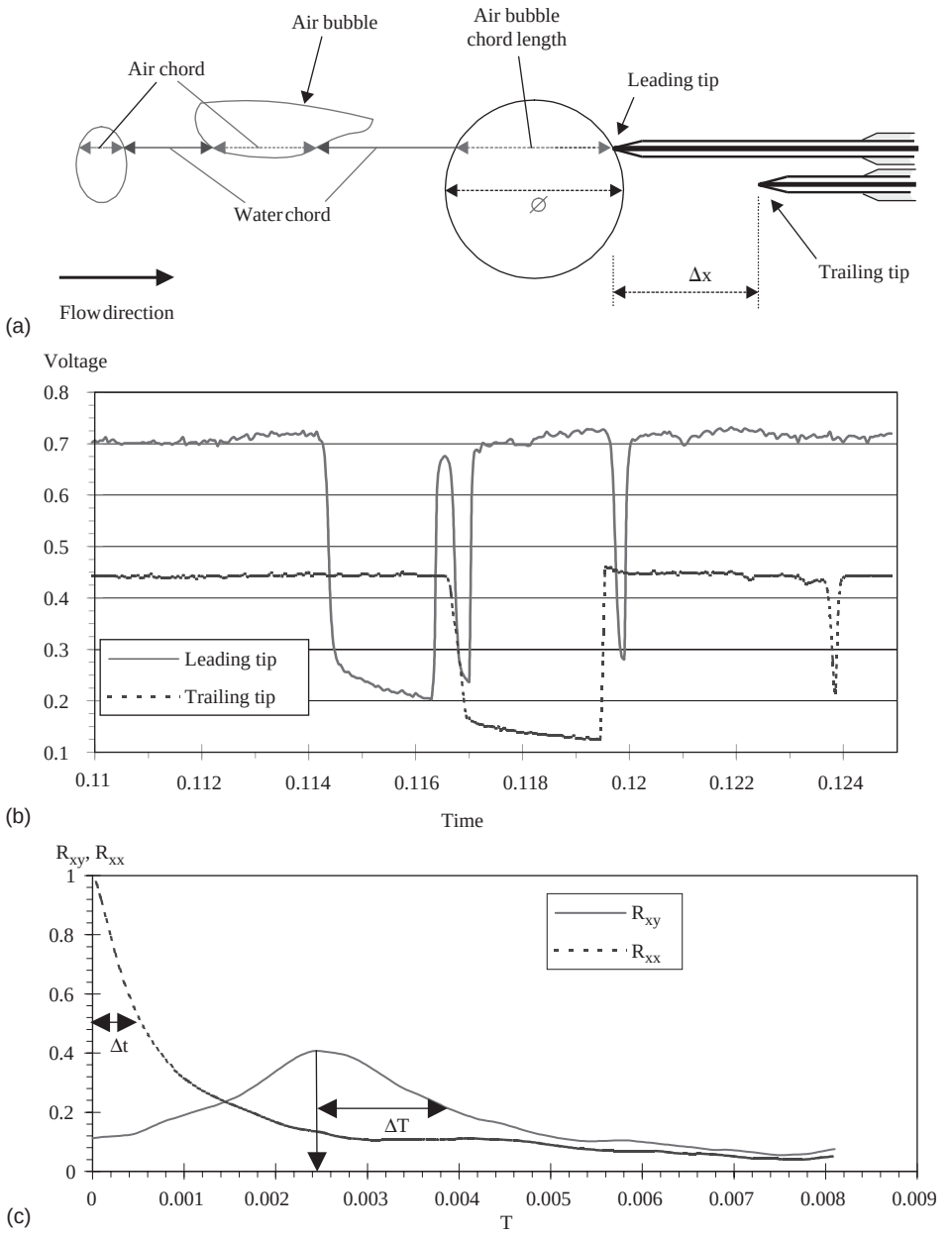

Figure 6. Local air–water flow measurements in skimming flow down a stepped chute (16° slope, $h = 0.10$ m, $d_c/h = 1.5$) with a double-tip conductivity probe (scan rate: 40 kHz per tip, $Ø = 0.025$ mm, $\Delta x = 8$ mm) – $C = 0.09$, $V = 3.05$ m/s, $F = 121$ bubbles per second, $y = 39$ mm, step 8. (a) Sketch of bubble impact on phase-detection probe tips (dual-tip probe design); (b) Voltage outputs from a double-tip conductivity probe; (c) Normalised auto-correlation and cross-correlation functions.

where Δx is the distance between tips and T is the time for which the cross-correlation function R_{xy} is maximum (Fig. 6C). The shape of the cross-correlation function provides further information on the velocity fluctuations (CHANSON and TOOMBES 2002). The turbulent intensity may be derived from the broadening of the cross-correlation function compared to the auto-correlation

function:

$$Tu = \frac{u'}{V} = 0.851 * \frac{\sqrt{\Delta T^2 - \Delta t^2}}{T} \quad (9)$$

where ΔT as a time scale satisfying: $R_{xy}(T + \Delta T) = 0.5\, R_{xy}(T)$, R_{xy} is the normalised cross-correlation function, and Δt is the characteristic time for which the normalised autocorrelation function R_{xx} equals 0.5 (Fig. 6C). The autocorrelation function R_{xx} provides some information on the air–water flow structure. A dimensionless integral length scale is:

$$I_L = 0.851 * \frac{\Delta t}{T} \quad (10)$$

A time series analysis gives information on the frequency distribution of the signal which is related to the air & water (or water & air) length scale distribution of the flow. Chord sizes may be calculated from the raw probe signal outputs. The results provide a complete characterisation of the streamwise distribution of air and water chords, including the existence of bubble/droplet clusters (e.g. CHANSON and TOOMBES 2002). The measurement of air–water interface area is a function of void fraction, velocity, and bubble sizes. The specific air–water interface area a is defined as the air–water interface area per unit volume of air and water. For any bubble shape, bubble size distribution and chord length distribution, it may be derived from continuity:

$$a = \frac{4 * F}{V} \quad (11)$$

where Equation (11) is valid in bubbly flows ($C < 0.3$). In high air content regions, the flow structure is more complex and the specific interface area a becomes simply proportional to the number of air–water interfaces per unit length of flow ($a \propto 2 * F/V$).

4 NEW DEVELOPMENTS IN AIR–WATER FLOW APPLICATIONS

While air–water flow measurements have been successfully conducted in models and prototypes, current techniques are limited to steady freshwater flows. In unsteady flows, the processing technique must be modified. Early experiments in seawater suggested that biochemicals, surfactants and living organisms interact with the flow turbulence and may affect drastically the air entrainment processes. Both issues are briefly discussed below.

4.1 *Unsteady flow measurements*

Air–water flow measurements in unsteady flows are difficult, although prototype observations of sudden spillway releases and flash floods highlighted strong aeration of the leading edge of the wave associated with chaotic flow motion and energy dissipation (Fig. 7). Figure 7A presents a flood wave advancing down the Brushes Clough dam stepped spillway. Figure 7B shows a laboratory experiment of dam break wave propagation down a stepped waterway.

In unsteady air–water flows, the measurement processing technique must be adapted (STUTZ and REBOUD 2000, CHANSON 2003), in recent experiments, local void fractions were calculated over a short time interval $\tau = \Delta X/C_s$ where C_s is the measured surge front celerity and ΔX is the control volume streamwise length. Measurements were conducted in a stepped chute at several locations X' measured from the vertical step face. Figure 8 shows dimensionless distributions of void fractions at $X' = 1.0$ m for several times $(t - t_s)$, where t_s is the time of passage of wave front. The legend indicates the control volume streamwise length ΔX and the dimensionless time $(t - t_s) * \sqrt{g/d_0}$, where d_0 is a measure of the initial flow rate $Q(t = 0+)$:

$$d_0 = \frac{9}{4} * \sqrt[3]{\frac{Q(t = 0+)^2}{g * W^2}} \quad (12)$$

and W is the channel width. For an ideal dam break, d_0 would be equivalent to the initial water depth behind the dam. The data are compared with corresponding steady flow data. The distributions of void fractions demonstrated a very strong aeration of the leading edge for $(t - t_s) * \sqrt{g/d_0} < 1.1$

to 1.3. In Figure 8, the data for $(t - t_s) * \sqrt{g/d_0} = 0.25$, 0.25, 0.455, 0.66 and 2.11 yielded depth-averaged void fractions $C_{mean} = 0.47$, 0.54, 0.40 and 0.25 respectively. In steady flow, the mean air content was $C_{mean} = 0.20$.

At the front of the wave, the void fraction distributions had roughly a linear shape:

$$C = 0.90 * \frac{y}{Y_{90}} (t - t_s) * \sqrt{g/d_0} < 1.2 \qquad (13)$$

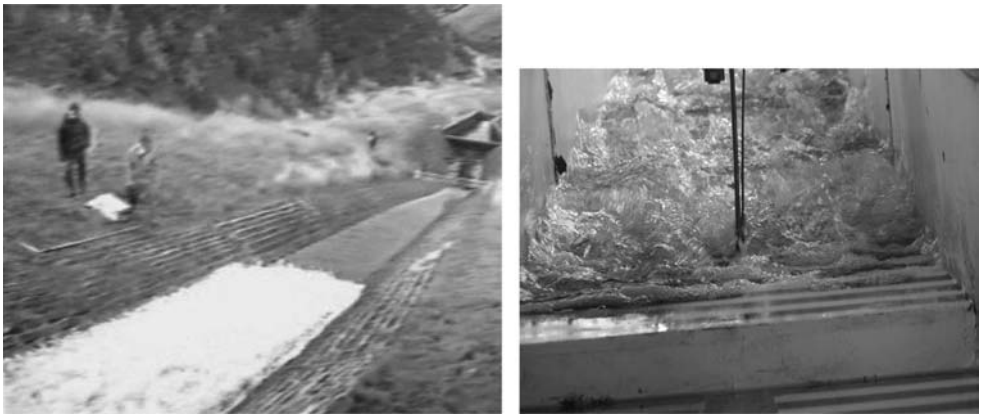

(a) (b)

Figure 7. Advancing flood waves down stepped chutes (leading edge of dam break waves); (a) Flood wave propagating down Brushes Clough dam spillway during field tests in 1994 (Courtesy of Dr R. BAKER) – $Q(t = 0+) \sim 0.5\ m^3/s$, 18.4° slope, $h = 0.19$ m; (b) Looking upstream at an advancing wave on step 16 with an array of conductivity probes in foreground – $Q(t = 0+) = 0.055\ m^3/s$, $d_o = 0.241$ m, 3.4° slope, $h = 0.07$ m ($W = 0.5$ m).

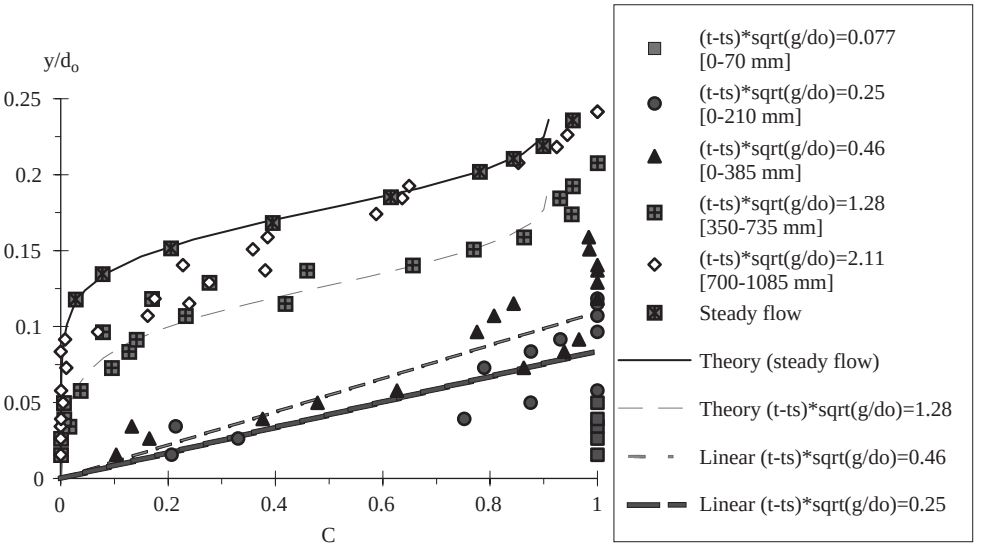

Figure 8. Dimensionless void fraction distributions behind the wave front leading edge ($Q(t = 0+) = 0.075\ m^3/s$, $d_o = 0.300$ m, $h = 0.07$ m, $l = 1.2$ m, Step 10, $C_s = 2.61$ m/s, $X' = 1.0$ m) – Comparison with steady flow data, and Equations (13) and (7).

where Y_{90} is the location where C = 90%. Equation (13) is a limiting case of the analytical solution of air bubble diffusion equation for steady transition flows down stepped chute (Eq. (6)). For larger times $(t - t_s)$, the distribution of air concentration may be described by a advective diffusion model (Eq. (7)). Equations (13) and (7) are plotted for steady and unsteady flow conditions in Figure 8. For all experiments, a major change in void fraction distribution shape took place for $(t - t_s) * \sqrt{g/d_0} \sim 1.1$ to 1.5. Possible explanations may include non hydrostatic pressure distributions at the leading wave front, some change in air–water flow structure associated with a change in rheological fluid properties, a change in gas-liquid flow regime, with a plug/slug flow regime in front a homogenous bubbly flow region behind, and some alteration in shear stress distributions and boundary friction.

Further air–water velocity measurements were conducted in the wave front. At the leading edge, instantaneous velocity measurements suggested a boundary layer region with a potential region above. The data showed however unusually large velocities at the leading edge, although the velocity distribution tended rapidly toward a quasi-steady flow pattern. At the leading edge, boundary layer velocity data were compared successfully with an analytical solution of the Navier-Stokes equations (first Stokes problem):

$$\frac{V}{U} = \text{erf}\left(\frac{y}{2 * \sqrt{\nu_T * (t - t_s)}}\right) \tag{14}$$

where U is the fre-stream velocity, ν_T is the kinematic viscosity, and y is the distance normal to the invert. Despite some scatter, the results suggested a turbulent boundary layer flow. The data yielded a ratio of air bubble diffusivity to eddy viscosity of about unity, implying very strong interactions between momentum transfer and air bubble diffusion processes.

4.2 *Air entrainment in seawater*

While most studies of air entrainment were conducted with freshwater, a small number of basic studies in seawater suggested that air entrainment may be an entirely different process, although the physical fluid properties are close (Table 1). Some studies considered the size of bubbles produced by a frit, showing that bubble coalescence was drastically reduced in saltwater compared to freshwater experiments (e.g. SCOTT 1975, WALKDEN 1999). Similar trends were recorded during wave flumes and tilting bucket experiments (BOWYER 1992, HAINES and JOHNSON 1995), although most works used visual observations implying very-low void fraction flow conditions.

An experimental study of developing flow region of plunging jets was conducted systematically with freshwater, seawater and salty freshwater (CHANSON et al. 2002). The results indicated lesser air entrainment in seawater than in freshwater, all inflow parameters being identical. It was hypothesised that surfactants, biological and chemical elements harden the induction trumpet and diminish air entrapment at impingement in seawater. Typical bubble sizes were millimetric in seawater with mean chords of about 3–6 mm. Seawater bubbly flows contained comparatively a greater number of fine bubbles than freshwater plunging jets for identical inflow conditions. These fine bubbles (less than 0.5 mm) have a slower rise velocity and they give a visual, misleading appearance to the air–water flow suggesting inaccurately that very fine bubbles are predominantly entrained in seawater plunging jets (Fig. 9).

Table 1. Measured physical properties of water solutions (after CHANSON et al. 2002).

Property (1)	Tap water (2)	Seawater (3)	Salty tap water (3.45% solution) (4)	Remarks (5)
Density (kg/m^3)	998.2	1,024	1,024	At 20° Celsius
Dynamic viscosity (Pa.s)	1.015 E-3	1.22 E-3	1.18 E-3	At 20° Celsius
Kinematic viscosity (m^2/s)	0.925 E-6	0.97 E-6	0.962 E-6	At room temperature (about 22°C)
Surface tension (N/m)	0.073	0.076	0.075	At room temperature (22°C)
Conductivity (μS/cm)	87.7	49,000	53,600	At 25° Celsius
pH	6.83	8.1	6.94	At room temperature (22°C)

Figure 9. Air bubble entrainment at circular plunging jet in seawater $d_n = 0.0125$ mm, $x_1 = 0.050$ m, $V_1 = 2.46$ m/s.

Air entrainment at plunging jets differed between saltwater and seawater with less air and smaller bubbles entrained in seawater. The results implied that classical dimensional analysis is incomplete unless physical, chemical and biological properties other than density, viscosity and surface tension are taken into account. Overall the study demonstrated that air entrainment in the Sea is a complicated process which cannot be modelled accurately in small-size wave flumes nor with fresh water experiments. It was hypothesised that organic matter might also play a role in inhibiting bubble entrainment in seawater while living organisms may interact with the flow turbulence.

5 SUMMARY AND CONCLUSION

There are two basic mechanisms of air entrainment: local/singular entrapment and interfacial aeration. In hydraulic structures, both phenomena are observed, and "white waters" may induce some flow bulking and drag reduction, and they may contribute to air–water mass transfer and prevention of cavitation damage. These issues must be properly understood by professionals and taken into account in modern design of hydraulic structures.

In hydraulic engineering, the void fraction (or air concentration) ranges typically from zero (clear-water) to 100% (pure air), and the prototype flows are highly turbulent. For such flow conditions, it is acknowledged that the most robust instrumentation is the intrusive phase-detection probe. The basic probe outputs include the void fraction, bubble count rate, time-averaged velocity and turbulence intensity. Further outputs include bubble and droplet chord size distributions, the streamwise distributions of bubbles and the air–water flow structure.

The same type of instrumentation maybe used in unsteady air–water flows and in seawater. In the latter case, preliminary results suggested that a different air–water flow structure in seawater.

ACKNOWLEDGMENTS

The writer thanks his past and present students Dr P.D. CUMMINGS, Carlos GONZALEZ, Chung-hwee "Jerry" LIM, Chye-guan SIM, Chee-chong TAN, York-wee TAN, Dr L. TOOMBES for their help and assistance.

REFERENCES

ANWAR, H.O. (1994). "Self-Aerated Flows on Chutes and Spillways – Discussion." *Jl of Hyd. Engrg.*, ASCE, Vol. 120, No. 6, pp. 778–779.

BACHALO, W.D. (1994). "Experimental methods in Multiphase Flows." *Intl Jl of Multiphase Flow*, Vol. 20, Suppl., pp. 261–295.

BOWYER, P.A. (1992). "The Rise of Bubbles in a Glass Tube and the Spectrum of Bubbles Produced by a Splash." *Jl of Marine Res.*, Vol. 50, pp. 521–543.

BRATTBERG, T., and CHANSON, H. (1998). "Air Entrapment and Air Bubble Dispersion at Two-Dimensional Plunging Water Jets." *Chemical Engineering Science*, Vol. 53, No. 24, Dec., pp. 4113–4127. Errata: 1999, Vol. 54, No. 12, p. 1925.

CAIN, P. (1978). "Measurements within Self-Aerated Flow on a Large Spillway." *Ph.D. Thesis*, Ref. 78–18, Dept. of Civil Engrg., Univ. of Canterbury, Christchurch, New Zealand.

CAIN, P., and WOOD, I.R. (1981). "Measurements of Self-aerated Flow on a Spillway." *Jl. Hyd. Div.*, ASCE, 107, HY11, pp. 1425–1444.

CHANSON, H. (1993). "Self-Aerated Flows on Chutes and Spillways." *Jl of Hyd. Engrg.*, ASCE, Vol. 119, No. 2, pp. 220–243. Discussion: Vol. 120, No. 6, pp. 778–782.

CHANSON, H. (1994) "Drag Reduction in Open Channel Flow by Aeration and Suspended Load." *Jl of Hyd. Res.*, IAHR, Vol. 32, No. 1, pp. 87–101.

CHANSON, H. (1995). "Air Bubble Entrainment in Free-surface Turbulent Flows. Experimental Investigations." *Report CH46/95*, Dept. of Civil Engineering, University of Queensland, Australia, June, 368 pages.

CHANSON, H. (1997). "*Air Bubble Entrainment in Free-Surface Turbulent Shear Flows*." Academic Press, London, UK, 401 pages.

CHANSON, H. (1999). "Turbulent Open-Channel Flows: Drop-Generation and Self-Aeration. Discussion." *Jl of Hyd. Engrg.*, ASCE, Vol. 125, No. 6, pp. 668–670.

CHANSON, H. (2002). "Very Strong Free-Surface Aeration in Turbulent Flows: Entrainment Mechanisms and Air–water Flow Structure at the "Pseudo" Free-Surface", in "*Interaction of Strong Turbulence with Free Surfaces*", *World Scientific*, Advances in Coastal and Ocean Engineering Series, Vol. 8, Singapore, M. BROCCHINI and D.H. PEREGRINE Ed., Vol. 8, pp. 65–98.

CHANSON, H. (2003). "Sudden Flood Release down a Stepped Cascade. Unsteady Air–water Flow Measurements. Applications to Wave Run-up, Flash Flood and Dam Break Wave." *Report CH51/03*, Dept of Civil Eng., Univ. of Queensland, Brisbane, Australia, 142 pages.

CHANSON, H., and MANASSEH, R. (2003). "Air Entrainment at a Circular Plunging Jet. Physical and Acoustic Characteristics." *Jl of Fluids Eng.*, Trans. ASME, Vol., July.

CHANSON, H., and TOOMBES, L. (2002). "Air-water Flows down Stepped chutes: Turbulence and Flow Structure Observations." *Intl Jl of Multiphase Flow*, Vol. 27, No. 11, pp. 1737–1761.

CHANSON, H., AOKI, S., and HOQUE, A. (2002). "Scaling Bubble Entrainment and Dispersion in Vertical Circular Plunging Jet Flows: Freshwater versus Seawater." *Proc. 5th Intl Conf. on Hydrodynamics ICHD 2002*, Tainan, Taiwan, H.H. HWUNG, J.F. LEE & K.S. HWANG Editors, pp. 431–436.

CROWE, C., SOMMERFIELD, M., and TSUJI, Y. (1998). "*Multiphase Flows with Droplets and Particles*." *CRC Press*, Boca Raton, USA, 471 pages.

CUMMINGS, P.D. (1996). "Aeration due to Breaking Waves." *PhD thesis*, Dept. of Civil Engrg., University of Queensland, Australia.

CUMMINGS, P.D., and CHANSON, H. (1997). "Air Entrainment in the Developing Flow Region of Plunging Jets. Part 2: Experimental." *Jl of Fluids Eng.*, Trans. ASME, Vol. 119, No. 3, pp. 603–608.

CUMMINGS, P.D., and CHANSON, H. (1999). "An Experimental Study of Individual Air Bubble Entrainment at a Planar Plunging Jet." *Chem. Eng. Research and Design*, Trans. IChemE, Part A, Vol. 77, No. A2, pp. 159–164.

ERVINE, D.A., and FALVEY, H.T. (1987). "Behaviour of Turbulent Water Jets in the Atmosphere and in Plunge Pools." *Proc. Instn Civ. Engrs., London*, Part 2, Mar. 1987, 83, pp. 295–314. Discussion: Part 2, Mar.–June 1988, 85, pp. 359–363.

ERVINE, D.A., McKEOGH, E.J., and, ELSAWY, E.M. (1980). "Effect of Turbulence Intensity on the rate of Air Entrainment by Plunging Water Jets." *Proc. Instn Civ. Engrs*, Part 2, June, pp. 425–445.

FALVEY, H.T. (1980). "Air-water Flow in Hydraulic Structures." *USBR Engrg. Monograph*, No. 41, Denver, Colorado, USA.

FALVEY, H.T. (1990). "Cavitation in Chutes and Spillways." *USBR Engrg. Monograph*, No. 42, Denver, Colorado, USA, 160 pages.

HAGER, W.H., and KRAMER, K. (2003). "Historical Development of Free-Surface Chute Aeration." *Proc. 30th IAHR Biennial Congress*, Thessaloniki, Greece, J. GANOULIS and P. PRINOS Ed., Vol. E, pp. 389–396.
HAINES, M.A., and JOHNSON, B.D. (1995). "Injected Bubble Populations in Seawater and Fresh water Measured by a Photographic Method." *Jl of Geophysical Res.*, No. 100, No. C4, pp. 7057–7068.
JONES, O.C., and DELHAYE, J.M. (1976). "Transient and Statistical Measurement Techniques for two-Phase Flows: a Critical Review." *Intl Jl of Multiphase Flow*, Vol. 3, pp. 89–116.
KELLER, R.J. (1972). "Field Measurement of Self-Aerated High Speed Open Channel Flow." *Ph.D. thesis*, Dept. of Civil Eng., Univ. of Canterbury, New Zealand.
KEULEGAN, G.H., and PATTERSON, G.W. (1940). "A Criterion for Instability of Flow in Steep Channels." *Trans. Am. Geophysical Union*, Pt II, Vol. 21, July 1940, pp. 594–596.
McCURDY, E. (1956). "The Notebooks of LEONARDO DA VINCI." *Jonathan Cape*, London, UK, 6th edition, 2 volumes.
McKEOGH, E.J. (1978). "A Study of Air Entrainment using Plunging Water Jets." *Ph.D. thesis*, Queen's University of Belfast, UK, 374 pages.
MATOS, J., SÁNCHEZ, M., QUINTELA, A., and DOLZ, J. (1999). "Characteristic Depth and Pressure Profiles in Skimming Flow over Stepped Spillways." *Proc. 28th IAHR Congress*, Graz, Austria, Session B14, 6 pages.
NEAL, L.S., and BANKOFF, S.G. (1963). "A High Resolution Resistivity Probe for Determination of Local Void Properties in Gas-Liquid Flows." *Am. Inst. Chem. Jl*, Vol. 9, pp. 49–54.
PLUMPTRE, G. (1993). "*The Water Garden*." *Thames and Hudson*, London, UK.
REIN, M. (1998). "Turbulent Open-Channel Flows: Drop-Generation and Self-Aeration." *Jl of Hyd. Engrg.*, ASCE, Vol. 124, No. 1, pp. 98–102. Discussion: Vol. 125, No. 6, pp. 668–670.
SCOTT, J.C. (1975). "The preparation of Water for Surface Clean Fluid Mechanics." *Jl of Fluid Mech.*, Vol. 69, part 2, pp. 339–351.
STEWART, W.G. (1913). "The Determination of the N in Kutter's Formula for Various Canals, Flumes and Chutes on the Boise Project and Vicinity." *Report on 2nd Annual Conf. on Operating Men*, USBR, Boise, Idaho, USA, Jan., pp. 8–23.
STRAUB, L.G., and ANDERSON, A.G. (1958). "Experiments on Self-Aerated Flow in Open Channels." *Jl of Hyd. Div.*, Proc. ASCE, Vol. 84, No. HY7, paper 1890, pp. 1890-1 to 1890-35.
STUTZ, B., and REBOUD, J.L. (2000). "Measurements within Unsteady Cavitation." *Experiments in Fluids*, Vol. 29, pp. 545–552.
TOOMBES, L. (2002). "Experimental Study of air–water Flow Properties on Low-Gradient Stepped Cascades." *Ph.D. thesis*, Dept of Civil Engineering, The University of Queensland.
VAN DE SANDE, E., and SMITH, J.M. (1973). "Surface Entrainment of Air by High Velocity Water Jets." *Chem. Eng. Science*, Vol. 28, pp. 1161–1168.
WALKDEN, M.J.A. (1999). "Model Wave Impulse Loads on Caisson Breakwaters: Aeration, Scale and Structural Response." *Ph.D. thesis*, University of Plymouth, UK, 250 pages.
WOOD, I.R. (1983). "Uniform Region of Self-Aerated Flow." *Jl Hyd. Eng.*, ASCE, Vol. 109, No. 3, pp. 447–461.
WOOD, I.R. (1984). "Air Entrainment in High Speed Flows." *Proc. Intl. Symp. on Scale Effects in Modelling Hydraulic Structures*, IAHR, Esslingen, Germany, H. KOBUS editor, paper 4.1.
WOOD, I.R. (1985). "Air Water Flows." *Proc. 21st IAHR Congress*, Melbourne, Australia, Keynote address, pp. 18–29.
WOOD, I.R. (1991). "*Air Entrainment in Free-Surface Flows*." *IAHR Hydraulic Structures Design Manual No. 4*, Hydraulic Design Considerations, Balkema Publ., Rotterdam, The Netherlands, 149 pages.